Experimental and numerical analysis of corrosion induced cover cracking in reinforced concrete beam

Benjamin Richard, Marc Quiertant, Véronique Bouteiller, Lucas Adelaide, Maxime Perrais, Jean-Louis Tailhan, Christian Cremona

EXPERIMENTAL AND NUMERICAL ANALYSIS OF CORROSION-INDUCED COVER CRACKING IN REINFORCED CONCRETE BEAM

Benjamin RICHARD[1], Marc QUIERTANT[1], Véronique BOUTEILLER[1], Lucas ADELAIDE[1], Maxime PERRAIS[1], Jean-Louis TAILHAN[1], Christian CREMONA[2]

[1]Univ. Paris-Est, French Public Works Laboratory, Paris, France.

Benjamin.Richard@lcpc.fr,

Marc.Quiertant@lcpc.fr, Veronique.Bouteiller@lcpc.fr,Lucas.Adelaide@lcpc.fr, Maxime.Perrais@lcpc.fr, Jean-Louis.Tailhan@lcpc.fr

[2]Ministry of Ecology, Energy, Sustainable Development and Sea, La Défense, France.

Christian.Cremona@developpement-durable.gouv.fr

Abstract

This paper aims to present both experimental and numerical studies of the corrosion induced cracking pattern evolution of a reinforced concrete sample subjected to accelerated corrosion. The sample was a concrete beam (1000x250x100 mm^3) reinforced with two rebars (20 mm diameter; 25 mm cover). The beam was not mechanically loaded. The corrosion process was applied on 500 mm rebar length on the central part. Rebars were intentiostatically corroded using a current density of 100µA/cm^2 of steel, in a chloride pond and for a thirty days period. Electrochemical tests (rest potentials, linear polarization resistance and impedance spectroscopy) and visual inspection were performed in order to characterize the rebar state (sound or corroded). Width evolution of the main longitudinal cover crack was measured thanks to ball-extensometer. A numerical modeling of the corroded RC beam has also been realized. The model allows taking into account the most important mechanisms such as the specific behaviour related to rust products. The proposed steel/concrete interface model has been recently developed by the authors and is based on damage mechanics. The experimental and numerical results are in good agreement and confirm the mean crack width induced by the iron oxide swelling. These results are very promising and indicate that this model could become a practical tool for civil engineers dealing with in-site repair and maintenance issues.

Keywords: reinforced concrete, corrosion, corrosion modeling, electrochemical characterization

1 Introduction

Stakeholders reported that corrosion could be considered as the main contributing factor of the performance degradation of existing reinforced concrete (RC) structures. Reinforcement corrosion leads to two important effects: the swelling of the iron oxides and the reduction of the rebar cross-section coupled with a decrease of its ductility. As a consequence of the first effect, tensile stresses appear on the rebar surrounding and concrete cover cracking may occur. In the cases of standard civil engineering building, first concrete cover cracks appear as soon as the corrosion phenomenon is developed enough. Therefore, it is of primary importance to provide to stakeholders and civil engineers powerful tools for predicting the development of the rebar corrosion. The aim of this paper is to present both experimental and numerical studies of the cracking pattern evolution of a RC beam subjected to accelerated corrosion. This study contributes to validate a steel/concrete interface constitutive model by comparison with experimental results, not only from a qualitative point of view but also from a quantitative one. To reach this objective, this paper is outlined as

follows. In section 2, the experimental program is exposed. Especially, the RC sample and the accelerated corrosion technique are introduced. In section 3, both mechanical and electrochemical results are exposed and discussed. In section 4, a numerical modeling of the experiment is proposed. The results are presented (damage patterns as well as a coarse estimation of the main crack opening) and discussed.

2 Experimental program

This section aims to introduce the experimental program that has been established and followed in order to carry out the present results.

2.1 Reinforced concrete beam description

The test specimen is a 1000 mm long RC beam with a 500x100 mm^2 rectangular cross section reinforced longitudinally with two 20 mm diameter steel deformed rebars. The concrete cover thickness is 25 mm. A schematic representation of the reinforcement concrete specimen is given in figure 1. The beam was not mechanically loaded. The cement type used is standard CEMI 52.5 PMES CP2 NF with a weight density equal to 340 $kg.m^{-3}$. The sand as well as the aggregates type is Bernière 0/4 and 6.3/20 respectively. The related weight densities are 739.45 $kg.m^{-3}$ and 1072.14 $kg.m^{-3}$. Water has been added to the mixture with a weight density equal to 184.22 $kg.m^{-3}$.

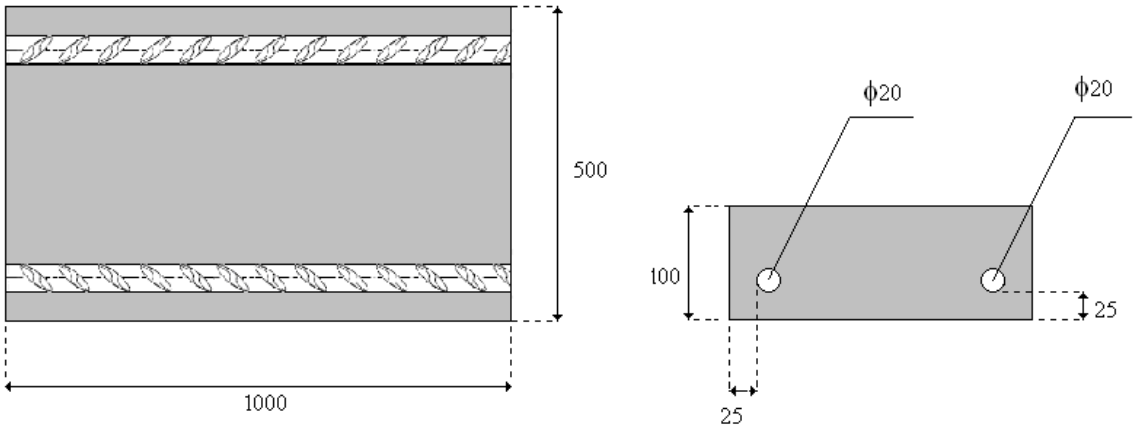

Figure 1. Geometry of the RC beam – (dimensions in mm).

2.2 Accelerated corrosion tests

The accelerated corrosion tests deal with placing the central part (500 mm) of the RC beam in a PVC tank containing an alkaline salted solution (1 $g.L^{-1}$ NaOH + 4.65 $g.L^{-1}$ KOH + 30 $g.L^{-1}$ NaCl), and polarizing the two rebars anodically using a counter electrode to enhance its corrosion. The counter electrode made of a Titanium platinum mesh (500 mm long, 250 mm wide) was placed at the bottom of the beam. A power supply delivered a constant current density of 100 $\mu A.cm^{-2}$ of steel between the rebars (connected to the positive pole) and the counter electrode (connected to the negative pole). The duration of the accelerated corrosion was thirty days (700 cumulated hours). Voltage, current and electrolyte level (100 mm height) were checked daily. This experimental set up adapted from the one proposed by Caré *et al.* [1] and Nguyen [2], leads to localise the corrosion process on the lower half part of the surface of the rebars (the bottom part of the rebars located in front of the counter electrode). A schematic representation of the accelerated corrosion testing setup is depicted in figure 2.

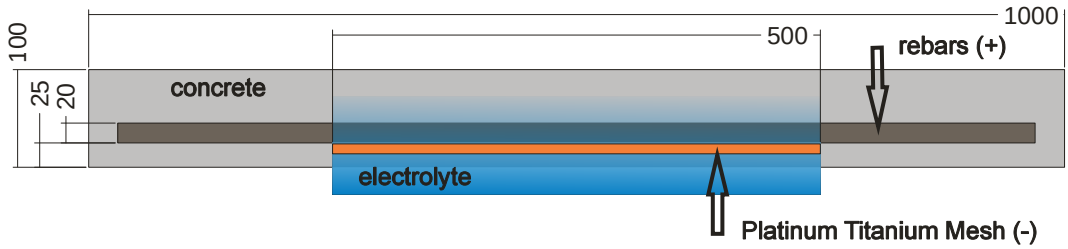

Figure 2. Scheme of the accelerated corrosion setup. The corroded area is located in the centre of the beam.

According to the Faraday's equation, the dissolved iron is equal to 96 µm:

$$\Delta r = \frac{MJt}{\rho zF} \quad (1)$$

where Δr is the theoretical steel cross section reduction (m), M the iron molar weight 55.85 10^{-3} kg.mol^{-1}), ρ the iron weight density (7,800 10^{3} kg.m^{-3}), J the prescribed current density (A.m^{-2}), z the valence number (equal to 2), F the Faraday's number (96,500 A.s^{-1}) and t the time (s).

2.3 Crack opening measurements

Crack opening measurements were performed using a "Pfender" extensometer (ball-extensometer). First of all, six pins were stuck on the studied face of the beam (see fig. 3). Pins are oriented by pair on a chosen generating line. The initial length between two pins of the same pair is set to about 10 cm. To limit initial ($t=t_0$) measurement uncertainties, each "absolute" value of spacing is in fact the result of the subtraction of the effective pins spacing and the measurement of an 10 cm invar gauge. The difference between the absolute spacing at a given time ($t \neq t_0$) and the initial absolute spacing characterizes the expansion along the generatrix. The energy released into the glue is assumed to be equal to zero. Therefore, the measured expansions are assumed to be due only to the concrete deformation process and crack opening. Figure 3 gives a picture of the pins location. The different possibilities of measurements are presented in figure 4.

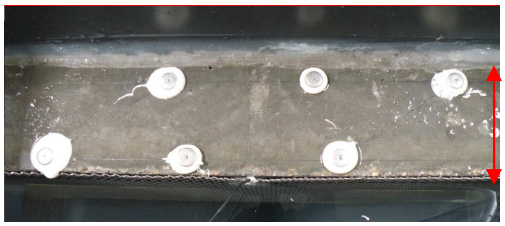

Figure 3. Picture of the sensors.

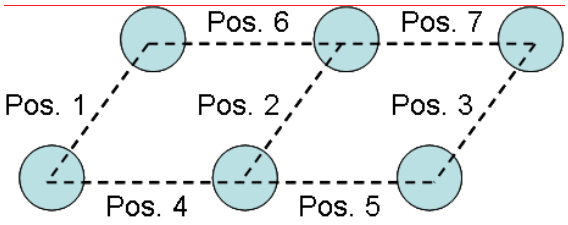

Figure 4. Positions of the measurements.

2.4 Electrochemical characterizations

The electrochemical system was composed of three electrodes: the working electrode was the steel rebars, the reference electrode was a KCl saturated calomel electrode (SCE) ($E°_{(NHE)}$=242 mV) and the counter electrode was a titanium/platinum-based grid. The electrolyte was salted water. The electrochemical measurements performed on the beam with a portable potentiostat PARSTAT PAR2263, were located on two different zones corresponding to rebars in the non corroded area and in the corroded area. The rest potential,

Ecorr (mV), was determined from the potential versus time curve, after ten minutes (the potential having reached its equilibrium). The impedance technique (frequency range from 100 kHz to 39 mHz) was used to determine both the concrete cover and the electrolyte resistance, R_e (Ohm), from the Nyquist diagram. The R_e value was taken as the real part of the impedance corresponding to the lowest point of the imaginary part of the impedance. From the linear polarization technique [3,4] (± 10 mV around the rest potential using a sweep rate of 2.5 mV.min^{-1}), the slope of the current versus voltage curve (1/(R_e + R_p)), was determined and the polarization resistance of the steel rebar, R_p (Ohm), was then calculated. The corrosion current density, Icorr (µA/cm²), (taking into account the ohmic drop and the polarised surface), was finally calculated based on the Stearn and Geary [5] equation (2):

$$I_{corr} = \frac{B}{R_p S} \tag{2}$$

with B a constant (26 mV), R_p (ohm) the polarization resistance and S (cm²) the polarized steel surface corresponding to the electrochemical cell design (126 cm² in this case).

3 Experimental results

In this section, the crack pattern and crack opening together with the corrosion characterizations are presented and discussed.

3.1 Crack pattern results

Due to the swelling related to the corrosion products, cracks starting from the steel/concrete interface and propagating towards the concrete cover appeared. Both crack pattern and crack opening were followed. The experimental results related to the quantitative cracking measurement are exposed in figures 5 and 6. In figure 5, the evolution of the crack opening versus the time is plotted. It can be mentioned that a bilinear relation linking the crack opening to the time seems to appear. Moreover, at the end of the accelerated test, the average crack opening related to the main longitudinal crack is equal to 139.10^{-6} m. In figure 6, strain measurements related to positions 4 to 7 have been reported. One can notice that the amplitude of the variations is very weak. From the experimental evidence, one can conclude that the swelling due to the corrosion products does not affect significantly the longitudinal direction. In other words, one can assess that the plane strain hypothesis is totally corroborated for a 2D calculation considering the cross section of the beam.

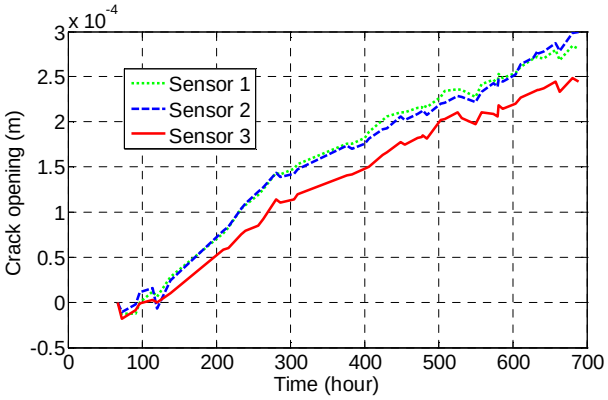

Figure 5. Crack opening versus time related to sensors 1, 2 and 3.

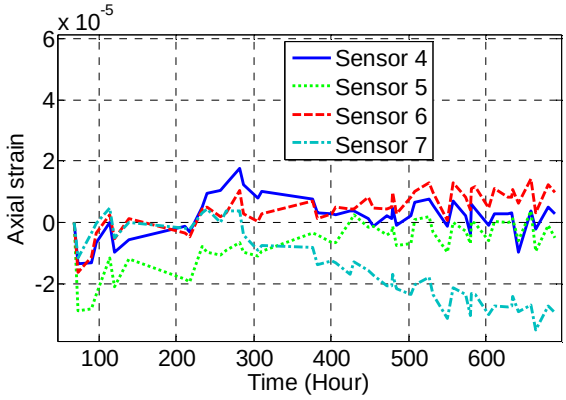

Figure 6. Strain evolution related to sensors 4-7.

3.2 Electrochemical results

The experimental results related to the rebar corrosion activity were reported in Table 1. Firstly, the potential values indicated that the corrosion probability of the rebar "R-in" was higher than the one of the rebar "R-out" because more negative. Secondly, the presence of chloride ions in the concrete was demonstrated by the much lower resistance of rebar "R-in" compared to rebar "R-out". Finally, concerning the corrosion current densities, the almost 18 $\mu A.cm^{-2}$ value for rebar "R-in" corresponding to a high level of corrosion compared to the 0.14 $\mu A.cm^{-2}$ value for the rebar "R-out" corresponding to a negligible - weak corrosion level (based on RILEM studies [6]) were conclusive in the characterization of two different rebar corrosion activities. All these results demonstrated the efficiency of the accelerated corrosion test.

Table 1 : Rebar corrosion activity characterizations

Location of the rebar	Potential, E_{corr} (mV, SCE)	Inverse of slope (ohm)	Resistance Re (ohm)	Corrosion current density, I_{corr} ($\mu A/cm^2$)
In the corroded area "R-in"	-0.622	217	205	17.96
Outside the corroded area "R-out"	-0.421	6,823	5,300	0.14

In order to confirm the non destructive electrochemical results, the RC beam was seen. The corroded rebar and the non corroded rebar can clearly be observed in figures 7.1 and 7.2 respectively.

Figure 7.1 Corroded rebar.

Figure 7.2 Non corroded rebar.

4 Numerical analysis

In this section, a numerical analysis of the reinforced concrete beam is presented. Firstly, the finite element (FE) modeling is described and secondly, the main results are shown and discussed.

4.1 Finite element modeling

The numerical analysis has been performed in order to study the predictive power of the constitutive models developed at French Public Works Laboratory (LCPC) [7-11]. Especially, a steel/concrete interface constitutive model has been recently developed and allows a fine description of local failure mechanisms due to the corrosion phenomenon. The reinforced

concrete specimen previously described has been found as being suitable for testing new models and constitutive laws. The aim of the numerical simulation is to estimate satisfyingly the crack opening and to predict the cracking pattern. The FE analysis lies in a two-dimensional model of the RC beam cross section. Due to the high transversal length (with respect to the other ones), the plane strain state hypothesis has been considered. This is consistent with experimental longitudinal strain measurement of the beam, as previously underlined. 25,142 three-node triangular finite elements have been used for meshing the domain occupied by the concrete. The FE mesh related to the constitutive concrete is shown in figure 8. It can be noticed that the mesh is rather fine, leading to a quite high computational cost. This choice has been made since an accurate cracking pattern is desired. If preliminary or non-detailed analyses had to be carried out, a coarser mesh could be used. The steel/concrete interface has been taken into account by meshing it by mean of zero-thickness elements.

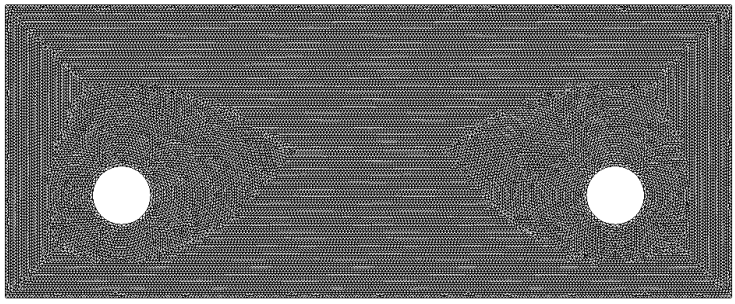

Figure 8. FE mesh used (only the part related to concrete).

In accordance with the experimental conditions, the vertical displacements related to the bottom line have been set up to zero. In order to avoid unwanted rigid modes, the right-bottom point has been built-in. In the present study, due to some random materials characteristics introduced over the concrete domain, FE modeling does not take advantage of the symmetry of the specimen. The concrete model used in the analysis has been proposed by Richard *et al.* [7] and has been implemented in the non commercial FE software Cast3M, supported by the Structural Mechanics Division of the French Atomic Research Center [12]. Cast3M is an open-source FE software and is devoted to both research and industrial applications. The concrete model used is based on damage mechanics. Therefore, a continuous description of the media is ensured. Nevertheless, the microcracking effects are taken into account thanks to a scalar damage variable, ranging from 0 (virgin materials) to 1 (broken materials). This variable makes the elastic modulus continuously vary between its initial value and 0. The proposed model is known for being able to tackle cyclic problems, involving an important contribution of hysteretic effects. Moreover, the so-called unilateral effect is taken into account partially, due to the scalar nature of the damage variable (see [7] for further explanations). The material parameters have been identified with respect to the experimental measurements performed on concrete specimens and are exposed in the table 2.

Table 2. Measured concrete properties.

Young's modulus	Poisson's ratio	Compressive strength	Tensile strength (splitting test)
36,500 MPa	0.21	44.7 MPa	3.3 MPa

Especially, a compression test has been performed on a concrete specimen. Both strains and stresses were monitored during the experiment in order to obtain the stress-strain curve. A

comparison between the experimental measurements and numerical results, at the Gauss' point level, is shown in figure 9.

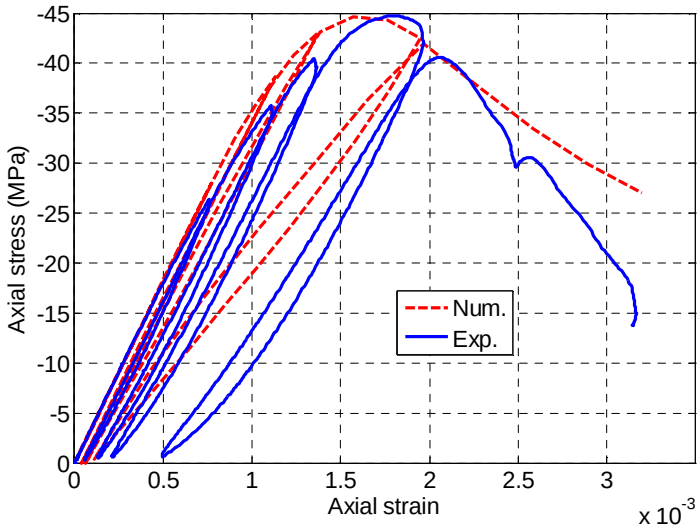

Figure 9. Experimental and calculated stress-strain curve

In order to take into account the concrete heterogeneity, the tensile stress has been sampled over the concrete domain (the mean value and the standard deviation have been identified with respect to the experimental measurements). In order to minimize the mesh-dependency effects, the well know non local approach has been used. The corresponding characteristic length has been set up to 13 mm, what corresponds to 2/3 times the maximum aggregate size. The steel/concrete interface model has been developed by Richard *et al.* [8]. Nevertheless, due to the fact that no mechanical loading is considered, all the possibilities offered by the model are not used (especially, the cyclic part and the steel-concrete bond loss). Internal pressure due to rust products from the corrosion process is modelled by prescribing a radial displacement at the steel/concrete interface. This is the only loading applied to the RC beam. The steel rebars have been assumed to behave elastically. The cross section reduction has not been taken into account since no mechanical loading is considered.

4.2 Numerical results

In this section, the numerical results obtained by mean of the model proposed by Richard *et al.* [8] are shown and discussed. The numerical damage pattern is exposed in figure 10. The only loading is swelling due to the presence of corrosion products. Therefore, the damage pattern that has been obtained is standard. The dissymmetry between both damage patterns around the two steel reinforcement bars is due to the concrete tensile strength sampled over the FE mesh to take into account its heterogeneity. In figure 11, a zoom in the bottom-left corner is presented.

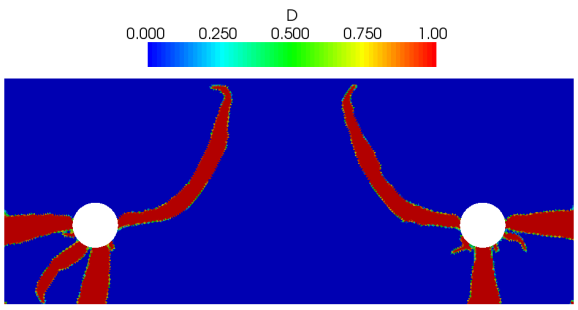

Figure 10. Numerical damage pattern.

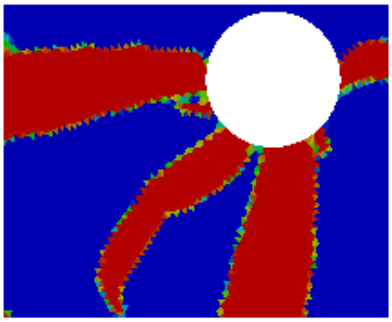

Figure 11. Zoom in the region of interest (bottom-left corner).

This qualitative numerical result can be compared to the experimental crack path. Figures 12 and 13 depict the experimental crack path in the longitudinal direction and from the cross section point of view respectively. These two pictures are focused on the left side of the beam. First, one can observe a main longitudinal crack. This crack has been satisfyingly captured by the numerical analysis. Second, from a cross sectional point of view, two cracks starting close the steel and propagating toward the concrete cover appeared (cf. figure 13). The numerical damage pattern shows one more crack (cf. figure 10). This difference can be explained by the fact that the computations have been carried out by considering a unique sample of the limit tensile stress distribution. Moreover, the concrete cutting showed that some granulates were very close to the steel/concrete interface what leads to highly influence the crack path. Therefore, it might have been interesting to sample various tensile stress distributions and then, to average the results in order to get a mean numerical response. This kind of analysis was not carried out because of the important computational time required. Smaller aggregates could also have been used. This choice has not been made because it is not very representative of in-site conditions.

Figure 12. Experimental crack path along the axial direction.

Figure 13. Experimental crack path in the cross section.

From a more quantitative point of view, a coarse estimation of the main crack opening was realized. Due to the continuous nature of the constitutive models used, an accurate determination of the crack openings could not be performed. Recently, non intrusive approaches have been developed in order to make possible a crack opening estimation combined with the use of continuum damage mechanics based models [11-13]. Especially, one of the simplest approaches lie in carrying out a FE computation and performing the difference between the nodal displacements in the regions of interest. The regions of interest are usually located where the damage variable is close to 1. If this condition is assumed to be fulfilled, displacements can occur but no stress will be created. Therefore, the displacements can be interpreted as crack openings, if the cohesive effects are assumed not to be of primary importance (pure mode I occurs). The latter approach was used in this study. The region of interest that was chosen is depicted in figure 11. By averaging the relative nodal displacements computed on the left boundary of the region of interest, one obtained a crack opening equal to 126.10^{-6} m, what is in accordance with the measured value (139.10^{-6} m). These results lead to conclude that the proposed constitutive models can be turned to handle practical engineering problems, allowing a fine crack description.

5 Conclusions and outlooks

In this paper, the results coming from both experimental and numerical investigations of corrosion-induced concrete cracking of a RC beam have been exposed. First, the specimen was subjected to an accelerated corrosion process in order to initiate concrete cover cracking. Both crack path and opening were followed versus time. Second, a numerical modeling RC

specimen has been proposed. The numerical modeling based on the FE method takes into account the constitutive models developed at LCPC. The numerical results were compared to the experimental ones and a satisfying agreement appeared not only qualitatively but also quantitatively. These results seem very promising and show that they can be turned to tackle engineering problems.

Acknowledgements

The investigations and results reported herein are supported by the National Research Agency (France) under the APPLET research program (grant ANR-06-RGCU-001-01)

References

[1] Caré S., Raharinaivo A. (2007) Influence of impressed current on the initiation of damage in reinforced mortar due to corrosion of embedded steel, Cement and Concrete Research, 37:1598-1612.

[2] Nguyen Q.T., Caré S., Millard A., Berthaud Y. (2007) An analysis of concrete cracking due to accelerated corrosion. Comptes Rendus Mécanique, 335:99-104. (in French).

[3] Wenger F. (1986) Etude de la corrosion de l'acier doux dans le béton par des méthodes électrochimiques – Application au contrôle des ouvrages de génie civil. PhD thesis. University of Paris Sud.

[4] Scully J.R. (2000) Polarization Resistance Method for Determination of Instantaneous Corrosion Rates. Corrosion, 56:199-217.

[5] Stern M., Geary A. (1957) A theoretical analysis of the shape of polarization curves, Journal of Electrochemical Society, 104:56.

[6] Andrade C., Alonso A. (2004) Test methods for on-site corrosion rate measurement of steel reinforcement in concrete by means of the polarization resistance method. Materials and Structures, 37:623-643.

[7] Richard B., Ragueneau F., Crémona C., Adelaide L. (2010) Isotropic continuum damage mechanics for concrete under cyclic loading: stiffness recovery, inelastic strains and frictional sliding. Engineering Fracture Mechanics, 77(8):1203-1223.

[8] Richard B., Ragueneau F., Crémona C., Adelaide L., Tailhan J.L. (2010) A three-dimensional steel-concrete interface model including corrosion effects. Engineering Fracture Mechanics, 77(6):951-973.

[9] Adelaide L., Richard B., Ragueneau F., Crémona C. (2010) Thermodynamical admissibility of a set of constitutive equations coupling elasticity, isotropic damage and internal sliding. Comptes Rendus Mécanique, 338:158-163.

[10] Ragueneau F., Richard B., Crémona C., Berthaud Y. (2010) Damage mechanics applied to the modeling of corroded reinforced concrete structures: steel, concrete and steel/concrete interface. European Journal of Environmental and Civil Engineering, 14(6-7):869-890.

[11] Richard B., Adelaide L., Cremona C. (2009) CEOS.FR French National Project Report.

[12] http://www-cast3m.cea.fr/cast3m/index.jsp

[13] Richard B., Ragueneau F., Delaplace A. (2010) Combining finite/discrete element methods: a postprocessing tool for fine crack description. International Journal of Solids and Structures. In submission.